ISSN 2723-6471

Iris Identification Using Resnet Iris Feature Extraction Architecture For Better Biometric Security

Hendi Sama[1,*], Tukino[2], Mangapul Siahaan[3], Erica Titoni[4]

[1,3,4]*Department. Information System, Faculty of Computer Science, Universitas Internasional Batam, Indonesia*

[2]*Department. Information System, Faculty of Creative Industries, Media Nusantara Citra University, Jakarta, Indonesia*

(Received: November 15, 2025; Revised: January 10, 2026; Accepted: March 15, 2026; Available online: April 18, 2026)

Abstract

Iris recognition is widely acknowledged as one of the most reliable biometric modalities due to its high uniqueness, rich textural patterns, and long-term stability. Unlike other biometric traits, iris characteristics resist forgery, aging effects, and environmental variations, making it suitable for high-security applications. Recently, convolutional neural networks (CNNs) have been extensively applied in iris recognition to improve feature representation and classification accuracy. However, many CNN-based approaches still depend on conventional segmentation and handcrafted features, which reduce robustness under noisy data, illumination variations, occlusions, or unconstrained environments. To address these limitations, this study proposes an enhanced iris identification framework combining a modified T-Net for precise segmentation with deep residual feature extraction for improved discrimination. Unlike conventional systems focus mainly on classification, the proposed approach emphasizes segmentation-driven feature consistency, ensuring extracted features originate from accurately localized iris regions. This design enhances stability and reliability, particularly under challenging imaging conditions. The framework leverages transfer learning and efficient representation learning strategies, enabling high accuracy even with a limited labelled data. Evaluations on three benchmark datasets CASIA-IrisV4, IITD Iris Database, and UBIRIS.v2 covering both controlled and less-constrained acquisition scenarios. Results show that it achieves classification accuracy of up to 98.35%, while maintaining computational efficiency suitable for deployment. The proposed architecture offers a robust, data-efficient, and scalable solution for secure biometric authentication, with strong potential for real-world applications such as access control, identity verification, and high-security authentication systems.

Keywords: Biometric Identification, Security Systems, Deep Learning, Convolutional Neural Networks, Computer Vision, Iris Recognition, Authentication

1. Introduction

With rising concerns about security and the need for robust data protection, compliance with security standards, and dependable authentication techniques, biometric systems have become increasingly important worldwide. Consequently, biometric identification technology is now deeply embedded in everyday life. This research introduces an innovative biometric recognition system that employs a deep learning approach to identify individuals using iris-based biometric data. In recent years, deep learning has greatly enhanced biometric technologies, achieving exceptional results across diverse applications. [1].

Deep learning algorithms have addressed numerous challenges posed by traditional machine learning, especially the need for manual feature extraction. Unlike classical approaches, deep learning models can autonomously handle biometric image transformations and derive relevant features directly from unprocessed data [2]. In the field of biometrics, many studies have incorporated machine learning and deep learning for identification tasks. Nevertheless, these methods often still depend on preprocessing stages to adapt raw biometric inputs into a form suitable for classification [3]

Traditional feature extraction methods face significant limitations, including inconsistent performance across different biometric modalities and even within datasets of the same biometric trait. These techniques are also often sensitive to

***Corresponding author: Hendi Sama (Hendi@uib.ac.id)**
DOI: https://doi.org/10.47738/jads.v7i2.1166

image transformations such as scaling and rotation, which can degrade their accuracy [4]. In comparison, deep learning-based approaches exhibit superior adaptability and robustness in managing such variations. Recent advances in deep learning have significantly improved biometric recognition systems by enabling automatic feature learning and end-to-end optimization. In iris recognition, CNN-based models have demonstrated superior performance in handling complex texture variations and non-linear feature representations compared to traditional handcrafted descriptors such as Gabor filters or wavelet-based methods. Residual learning architectures, in particular, have shown strong capability in preserving discriminative information across deep layers, leading to improved robustness against illumination changes, occlusions, and noise. This method has evolved into one of the most reliable biometric identification systems, employing sophisticated pattern analysis algorithms to interpret the distinctive textural characteristics of the iris. With the proliferation of digital devices including smartphones, tablets, computers, and wearable technology in the 21st century, there has been a dramatic surge in the storage of personal digital content. This escalation in sensitive data storage has correspondingly increased the demand for secure authentication methods, positioning iris recognition as a critical security solution [5].

Anatomically, the front part of the eye consists of three main structures: the pupil, iris, and sclera. The iris, positioned between the dark pupil and the white sclera, displays unique morphological characteristics such as crypts, furrows, and a trabecular meshwork that vary from person to person these patterns even differ between the left and right eyes of the same individual. This high level of variability makes the iris an ideal biometric identifier. Unlike external biometric traits such as facial features or hand geometry, the iris offers distinct advantages as an internal yet visible structure that maintains its form throughout a person's lifetime, showing remarkable resistance to age-related changes or physical alterations. A standard iris recognition system generally consists of six main stages, namely image acquisition, preprocessing, segmentation, normalization, feature extraction, and pattern matching [6]

To enhance the precision of iris identification, this study focuses on capturing distinctive texture patterns through an innovative multi-resolution and multi-domain analysis approach. The proposed technique integrates powerful feature extraction methods, combining gradient-based descriptors like HOG with advanced neural network models including T-Net architecture. These specialized convolutional networks dramatically improve processing speed by effectively compressing iris feature data while preserving critical discriminative information [7].

In the verification stage, the system conducts pattern comparison between iris templates using enhanced correlation measurement techniques [8]. The authentication protocol utilizes binary feature matching to generate verification decisions (match/non-match). A key innovation is our refined implementation of the ORB (Oriented FAST and Rotated BRIEF) method, specially adapted for iris recognition tasks, which achieves superior processing speed without compromising recognition reliability [9].

2. Literature Review

Recent advancements in biometric systems have positioned iris recognition as one of the most reliable and secure identification methods due to its high uniqueness and stability over time. In the literature, traditional iris recognition approaches primarily rely on handcrafted feature extraction techniques such as Gabor filters, wavelet transforms, and texture descriptors. While these methods have demonstrated acceptable performance under controlled environments, they often suffer from limited robustness when dealing with noise, illumination variations, and occlusions. Additionally, their dependency on manual feature engineering restricts adaptability across diverse datasets and real-world scenarios [10].

With the emergence of deep learning, particularly Convolutional Neural Networks (CNNs), iris recognition systems have undergone significant transformation. CNN-based approaches enable automatic feature learning and hierarchical representation, allowing models to capture complex iris texture patterns more effectively than conventional techniques. Several studies have successfully applied well-known architectures such as ResNet, VGG, and MobileNet to improve classification accuracy and generalization performance. Moreover, transfer learning strategies have been widely adopted to address the challenge of limited labeled data, demonstrating promising results across multiple benchmark datasets [11].

Despite these advancements, the existing literature reveals several critical limitations. First, many studies treat iris segmentation and feature extraction as separate and independent stages. This pipeline design often leads to error

ISSN 2723-6471

propagation, where inaccuracies in segmentation negatively affect feature quality and overall recognition performance [12]. Second, most CNN-based approaches focus heavily on improving classification accuracy while overlooking the importance of segmentation quality, which is a crucial factor in ensuring that extracted features originate from the true iris region. Third, deep architectures such as ResNet, although powerful, tend to require high computational resources, making them less suitable for real-time or resource-constrained environments. Furthermore, existing methods often struggle to maintain robustness under unconstrained conditions, such as motion blur, occlusion, and non-uniform illumination, which are common in real-world applications [13].

Based on these limitations, a clear research gap can be identified. There is a need for an integrated, segmentation-aware iris recognition framework that not only improves classification performance but also ensures accurate localization of the iris region. Additionally, the system should be computationally efficient and capable of maintaining high performance even with limited training data and challenging imaging conditions. To address this gap, this study proposes a novel segmentation-aware iris recognition framework that combines a modified T-Net architecture for precise iris segmentation with deep residual feature extraction. Unlike conventional approaches that prioritize classification, the proposed method emphasizes the interdependency between segmentation and feature extraction to enhance feature consistency and robustness. Furthermore, by leveraging transfer learning and optimized network design, the proposed framework aims to achieve high accuracy while maintaining computational efficiency, making it suitable for practical biometric applications in real-world environments.

3. Methodology

3.1. Research Design

This study employs an experimental and quantitative research design to develop a robust iris recognition system based on deep learning. The proposed approach (figure 1) emphasizes a segmentation-aware pipeline, where accurate iris localization directly influences feature extraction and classification performance.

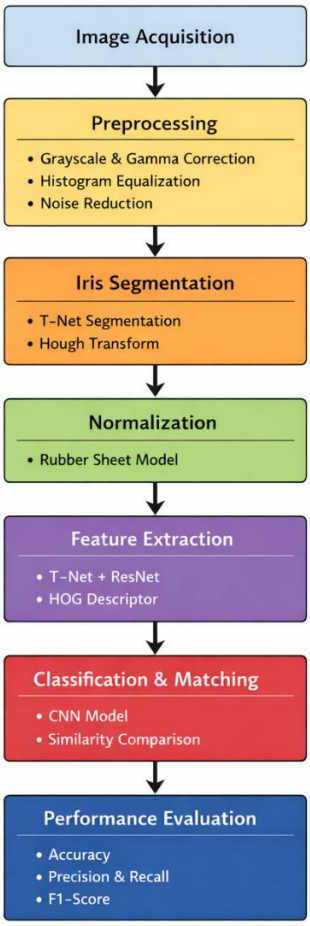

Figure 1. Research Framework

3.2. Dataset Description

The data used in this research were obtained from publicly available iris datasets, such as CASIA-Iris and IITD Iris Database, which were pre-processed and augmented to enhance feature extraction. The dataset used in this study primarily consists of high-resolution iris images captured under controlled conditions. Each iris sample is processed to extract distinct biometric features, with images serialized into standardized formats for deep learning analysis. To optimize computational efficiency, the dataset undergoes preprocessing, including normalization, noise reduction, and region-of-interest (ROI) cropping, ensuring consistent input quality for the ResNet-based feature extraction model. It is shown in table 1.

Table 1. Iris Dataset Composition

No	Dataset Source	Number of Images
1	CASIA-IrisV4	369
2	IITD Iris Database	374
3	UBIRIS.v2	420
	Amount	1163

The datasets vary in image resolution, capture conditions, and noise levels. CASIA and IITD datasets were captured under controlled near-infrared illumination, while UBIRIS.v2 contains visible-light images with higher noise, occlusion, and illumination variation. The datasets are class-balanced at the subject level to ensure fair evaluation.

3.3. Data Preprocessing

Iris image preprocessing has been widely recognized as a crucial stage in biometric recognition systems. Prior studies highlight that its primary objectives include noise reduction, enhancement of discriminative iris features, and simplification of data for subsequent processing stages. Effective preprocessing ensures that iris images are standardized and possess consistent region representation, which is essential for reliable feature extraction and matching. In the context of full facial images, the literature emphasizes the importance of accurate ocular region localization as an initial step. Various approaches have been proposed, including image filtering techniques to improve the signal-to-noise ratio and edge detection methods to facilitate precise iris boundary delineation. These preprocessing strategies collectively contribute to improving the robustness and accuracy of iris recognition systems [14].

3.3.1. Image Filtering

The preprocessing pipeline for iris images typically begins with essential filtering operations that prepare the data for subsequent edge detection and segmentation. This stage is widely acknowledged in the literature as crucial for reducing acquisition noise, normalizing illumination variations, enhancing edge structures, and improving overall image contrast, often through techniques such as histogram equalization. Filtering methods operate by manipulating different frequency components of the image, either attenuating noise in low-frequency regions or preserving high-frequency details that are important for feature extraction. Various studies have explored the effectiveness of spatial domain filters, such as mean and Gaussian filters, as well as more advanced operators, each offering different trade-offs between noise suppression and detail preservation. The selection of an appropriate filtering strategy has a significant impact on the robustness and accuracy of iris localization and subsequent recognition stages, as it directly influences the quality of the processed image used for further analysis [15]. The choice of filtering approach significantly impacts detection accuracy, with spatial domain filters (Mean, Gaussian) and advanced operators (exponential) offering different trade-offs between noise suppression and feature preservation. Properly executed filtering establishes the foundation for reliable iris localization and subsequent processing stages. For a given exponent value r, calculate the transformed pixel intensity P_{out} from the original pixel value P_{in} using the following exponential transformation equation:

$$P_{out} = 255 * \left(\frac{r}{2}\right) \quad (1)$$

The preprocessing stage begins with an exponential transformation (γ=0.45) applied to grayscale iris images, designed to non-linearly enhance contrast while preserving critical texture details. This gamma correction operation follows the power-law relationship I' = I^γ, where input intensities I are normalized to the [0,1] range before transformation. Histogram analysis provides quantitative validation, with comparative plots generated for both original and transformed images to visualize the intensity redistribution effect. Subsequently, histogram equalization is performed on UBIRIS v2 database images to optimize global contrast. The equalization process involves: (1) computing the discrete histogram h(i) for intensity levels i∈[0,255], (2) deriving the cumulative distribution function CDF(i) = (∑h(j) for j=0→i) × 255/N, where N represents the total pixel count, and (3) remapping intensities using the normalized CDF

ISSN 2723-6471

[16]. This cascaded enhancement approach effectively normalizes illumination variations while amplifying discriminative iris patterns crucial for accurate recognition:

$$\mathrm{CDF}(i) = \frac{1}{N}\sum_{k=0}^{i} h(k) \tag{2}$$

Histogram equalization (figure 2) is a contrast enhancement technique performed through a series of systematic steps. The process begins by computing the image histogram, which represents the number of pixels at each grayscale intensity level. Next, the histogram is normalized by dividing each intensity frequency by the total number of pixels, resulting in the Probability Density Function (PDF). The subsequent step involves calculating the Cumulative Distribution Function (CDF), which is obtained by cumulatively summing the PDF values from the lowest intensity level up to a given intensity. This CDF serves as the basis for the transformation function used to map original intensity values to new ones, typically by scaling the CDF with the maximum available intensity level. Once the transformation function is defined, each pixel in the image is repl aced with its corresponding new intensity value. As a result, the intensity distribution becomes more uniform, leading to improved image contrast and enhanced visibility of details, particularly in regions with low illumination. [17].

The implementation reveals how sequential application of gamma correction followed by histogram equalization synergistically enhances iris features while maintaining critical anatomical details. This preprocessing stage ensures subsequent feature extraction algorithms receive optimized input with improved signal-to-noise characteristics.

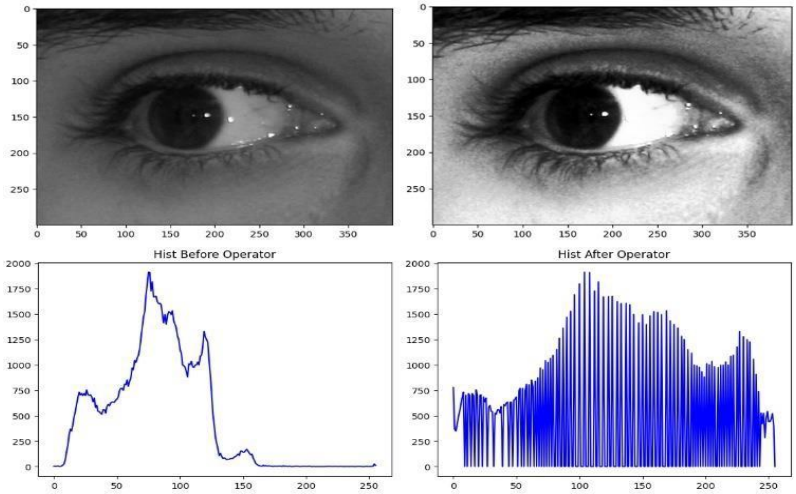

Figure 2. Histogram Equalization Implementation

Histogram equalization is a contrast enhancement technique performed through a series of systematic steps. The process begins by computing the image histogram, which represents the number of pixels at each grayscale intensity level. Next, the histogram is normalized by dividing each intensity frequency by the total number of pixels, resulting in the Probability Density Function (PDF). The subsequent step involves calculating the Cumulative Distribution Function (CDF), which is obtained by cumulatively summing the PDF values from the lowest intensity level up to a given intensity. This CDF serves as the basis for the transformation function used to map original intensity values to new ones, typically by scaling the CDF with the maximum available intensity level. Once the transformation function is defined, each pixel in the image is replaced with its corresponding new intensity value. As a result, the intensity distribution becomes more uniform, leading to improved image contrast and enhanced visibility of details, particularly in regions with low illumination.

The research employs a cascaded noise reduction strategy, initiating with a mean-based denoising step and subsequently applying Gaussian blurring. The initial noise suppression stage utilizes a square 9×9 averaging window that processes the image matrix through discrete convolution, substituting each target pixel with the mean intensity of its local 81-pixel vicinity. This spatial domain averaging operation successfully attenuates salt-and-pepper noise components while maintaining fundamental image characteristics, albeit with potential smoothing of sharp transitions at boundary regions. Building upon this initial smoothing, we apply a Gaussian filter - a sophisticated low-pass operator that weights neighbouring pixels according to a normal distribution. Unlike the uniform weighting of the mean filter, the Gaussian kernel assigns decreasing weights proportional to distance from the centre pixel, expressed mathematically through its two-dimensional coefficient function. This dual-stage filtering strategy progressively

suppresses noise across different frequency bands while maintaining optimal trade-offs between noise removal and feature preservation, particularly crucial for maintaining iris texture details in biometric applications [18].

The two-dimensional Gaussian kernel is mathematically defined by the equation $G(x,y) = (1/2\pi\sigma^2)\exp(-(x^2+y^2)/2\sigma^2)$, where x and y represent pixel coordinate offsets from the filter centre, and σ denotes the standard deviation controlling the smoothing intensity. In this study, we employed σ=0.8 for primary noise reduction while preserving critical iris texture features. Figure 3 demonstrates the visual outcome of applying a stronger Gaussian variant (σ=1.15), showing enhanced smoothing effects suitable for suppressing high-frequency noise in challenging acquisition conditions.

$$G(x,y) = \frac{1}{2\pi\sigma^2}e \tag{3}$$

The Gaussian filter's distance-weighted averaging provides superior edge-preserving smoothing compared to uniform mean filters, as nearby pixels contribute more significantly to the output than distant ones. This selective weighting mechanism makes it particularly effective for iris image preprocessing, where maintaining structural integrity while reducing noise is paramount for accurate biometric recognition [19].

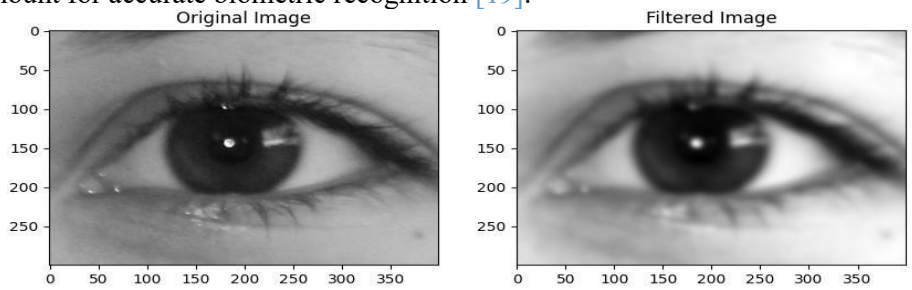

Figure 3. Gaussian filtering

3.3.2. EDGE Detection

Edge detection is a fundamental technique in image processing used to identify object boundaries by detecting significant changes in image intensity. It plays a vital role in iris recognition systems, as accurate boundary detection is essential for isolating the pupil and iris regions. Edges typically occur at transition points between distinct regions, and in iris images, they correspond to noticeable local variations in pixel intensity[20].

Various edge detection approaches have been extensively studied in the literature, including gradient-based methods and multi-stage detection techniques, each offering different levels of sensitivity to noise and localization accuracy. In addition to edge detection, the literature highlights the importance of geometric modeling for representing object boundaries, particularly in cases where structures exhibit regular shapes such as circular or elliptical forms. Geometric representations enable more precise characterization of boundaries and support robust analysis across varying imaging conditions. Furthermore, shape-based analysis techniques, including circular and elliptical modeling, have been widely applied in diverse domains such as biomedical imaging, agriculture, and object recognition, demonstrating their effectiveness in capturing structural properties of both natural and artificial objects. These approaches collectively contribute to improving the reliability and accuracy of boundary detection in complex image processing tasks [21]. Such techniques facilitate the examination of various natural and man-made objects ranging from cereal grains and produce (onions, melons) to biological specimens (cells, tissues) and facial recognition systems. In our implementation, we employ elliptical modelling for precise iris boundary delineation, as demonstrated in figure 4. The governing mathematical formulation appears as follows:

$$\frac{(x-h)^2}{a^2} + \frac{(y-k)^2}{b^2} \tag{4}$$

(h, k) is the centre of the ellipse, and $2a$ and $2b$ are the lengths of the axes of the ellipse. The longer axis is called the major axis, while the shorter axis is called the minor axis.

ISSN 2723-6471

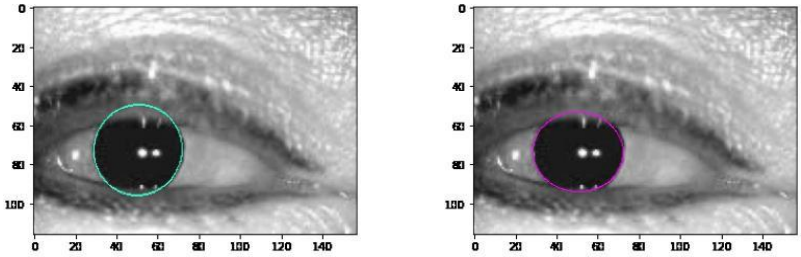

Figure 4 Ellipse Fitting iris Edge Detection

The Canny edge detector was then applied, which operates as a Gaussian first-derivative filter. This method is designed to maximize the Signal-To-Noise Ratio (SNR), making it highly effective for edge detection. As illustrated in figure 5, the Canny algorithm proves particularly suitable for identifying the pupil's edges. Additionally, it enhances the detection of the iris's outer boundary, which is often difficult to distinguish under normal conditions [22].

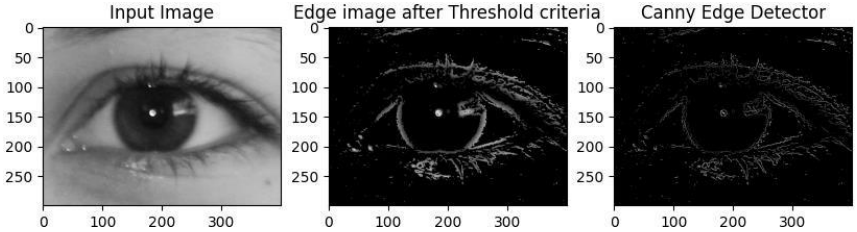

Figure 5. Iris edge detection by Canny edge detection

The Hough Transform represents a fundamental methodology in computer vision for identifying parametric shapes including linear structures, circular forms, and other mathematically definable contours. Initially conceptualized by Paul Hough during the early 1960s, this algorithm was specifically created to locate and characterize linear features in digital images, demonst rating particular efficacy when processing binary (black-and-white) image data. The core functionality of this approach lies in its ability to accurately pinpoint the spatial coordinates and geometric parameters of detected shapes [23].

Circle detection via the Hough Transform demonstrates greater computational efficiency compared to line identification. This efficiency stems from the straightforward mapping of circular parameters into Hough space, mirroring the operational principles of its linear counterpart. The mathematical representation requires only three parameters: radius (r) and the centre coordinates (a,b) along the x and y axes. Consequently, the parametric equation defining circular boundaries can be formulated as:

$$r^2 = (x - a)^2 + (x - b)^2 \tag{5}$$

However, as the number of parameters needed to define a shape increases, so does the dimensionality of the parameter space. This, in turn, raises the computational complexity of the Hough transform. By increasing the number of parameters required to describe the shape and similarly the dimensions of the spaceR parameter increase, likewise the complexity of the Hough transform. We have been used Hough transform in order to detect the iris outer and inner boundary as the result is demonstrated in figure 6.

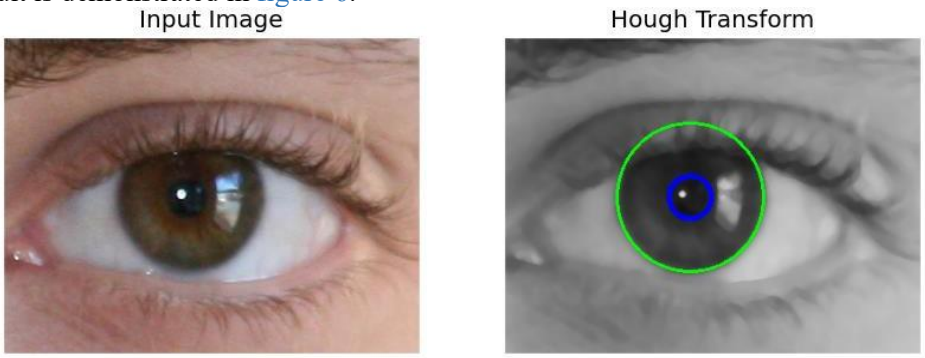

Figure 6. Hough Transform iris outer and inner boundary detection.

3.4. Iris Image Segmentation

Although U-Net has been widely adopted for biomedical image segmentation due to its effective encoder–decoder structure and skip-connection mechanism, several studies have reported limitations when dealing with objects that

ISSN 2723-6471

exhibit circular structures and low-contrast boundaries, such as those found in iris images. These challenges have motivated the exploration of alternative or modified network architectures that enhance feature representation and boundary continuity. In the literature, variations of convolutional neural network architectures have been proposed to address such limitations by incorporating deeper layers and improved feature aggregation strategies. These adaptations aim to better capture fine-grained structural details while maintaining computational efficiency. Consequently, the selection of an appropriate segmentation architecture plays a crucial role in achieving accurate and robust iris boundary detection, particularly under challenging imaging conditions [24], [25]. It is illustrated in figure 7 and figure 8.

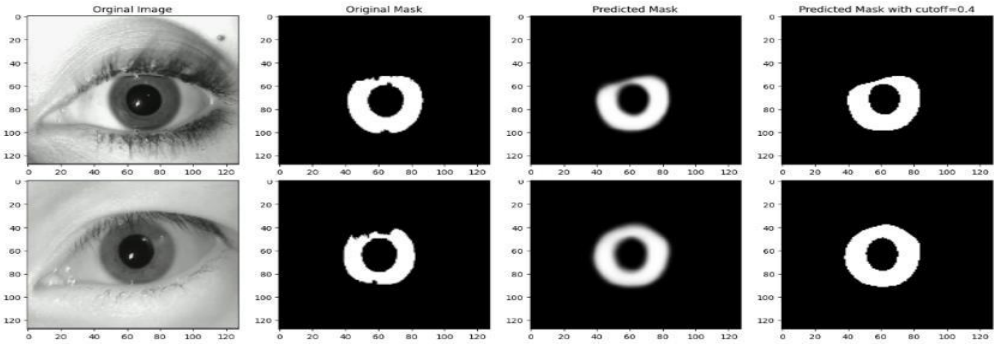

Figure 7 The result of Iris Segmentation using T-Net

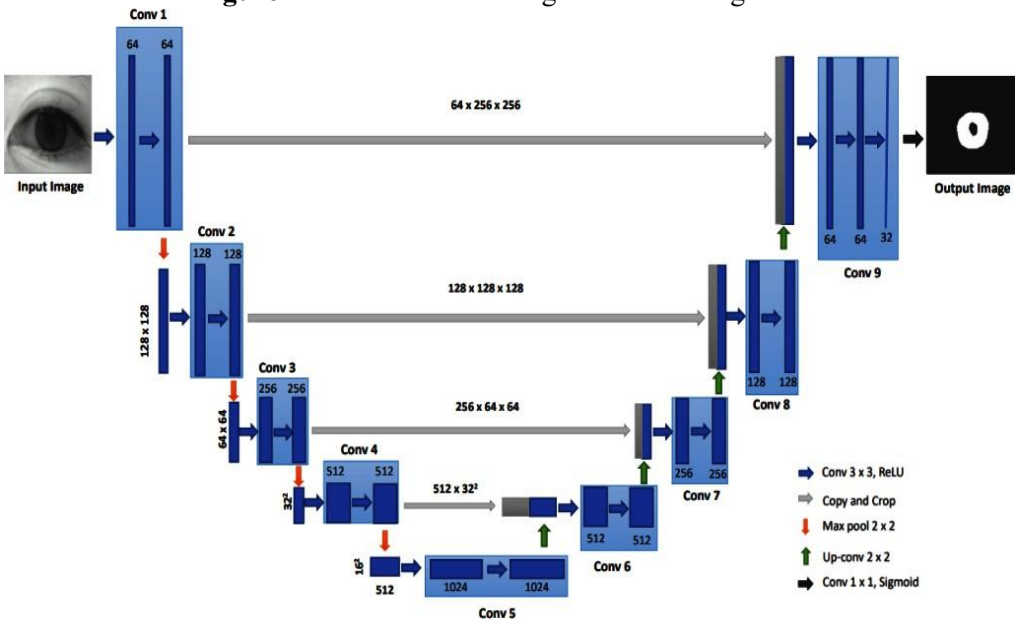

Figure 8. T-Net Structure used for Iris Image Segmentation

3.5. Iris Image Normalization

Iris images often exhibit variability in size, capture distance, and illumination conditions, resulting in differences in pupil diameter and overall brightness. To address these inconsistencies, normalization has been widely recognized as a critical step in iris recognition systems. The literature emphasizes that normalization aims to standardize the representation of the iris region, enabling consistent and reliable feature extraction across different samples. By compensating for variations caused by imaging conditions, pupil dilation, eye rotation, and head positioning, normalization techniques help reduce intra-class variability while preserving distinctive iris patterns. Various approaches have been proposed to achieve this objective, focusing on transforming the segmented iris region into a uniform representation that facilitates subsequent analysis. Consequently, normalization plays a fundamental role in improving the robustness and accuracy of iris recognition systems under diverse acquisition conditions [26]. For normalization, the Hough transform algorithm first identifies the iris's inner and outer boundaries. Subsequently, Daugman's Rubber Sheet Model is applied - a technique developed by John Daugman that maps iris points to polar coordinates (r, θ). Here, r represents the normalized radial distance [0,1], while θ denotes the angular position [0,2π]. The transformation from Cartesian (x,y) coordinates to this normalized polar system is achieved through the following mathematical representation:

 ISSN 2723-6471

$$I[x(r,\theta), y(r,\theta)] \rightarrow I(r,\theta) \quad (7)$$
$$x(r,\theta) = (1-r)\, x_p(\theta) + r\, x_l(\theta) \quad (8)$$
$$y(r,\theta) = (1-r)\, y_p(\theta) + r\, y_l(\theta) \quad (9)$$

In this representation, I(x,y) denotes the iris region in Cartesian coordinates, while (r,θ) represents the transformed polar coordinates. The variables (x_p,y_p) and ($x_ı$,$y_ı$) correspond to the pupil and iris boundary positions along the θ axis, respectively. The detection process identifies these boundaries by locating two approxim ately concentric circular edges - the inner boundary between pupil and iris, and the outer boundary between iris and sclera [27].

Figure 9 visually demonstrates this normalization process: the left panel shows the original image with detected boundaries, the centre displays the segmented iris region, and the right panel presents the final normalized iris image. This transformation effectively converts the annular iris region into a standardized rectangular format suitable for subsequent analysis.

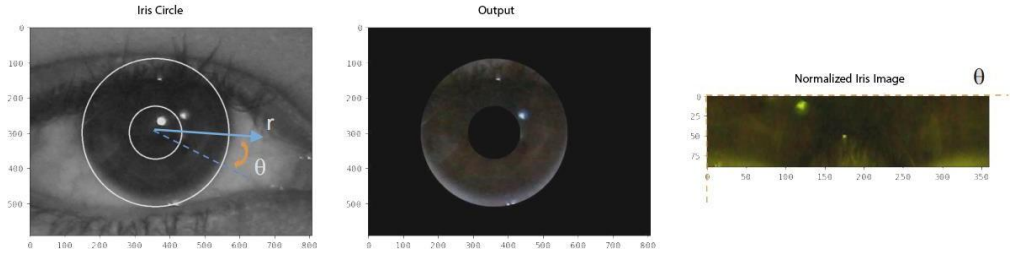

Figure 9. The Normalized iris image

The advancement of deep convolutional neural networks has led to the widespread adoption of Batch Normalization (BN), which applies normalization principles to intermediate network layers. Within the deep learning community, there is broad consensus that BN offers multiple benefits: it accelerates model training, permits the use of higher learning rates, and enhances generalization performance. This technique has become ubiquitous across virtually all deep learning applications [28].

BN improves gradient flow through the network by reducing the sensitivity of gradients to parameter scales or initial values. This stabilization enables the use of significantly higher learning rates without risking training divergence. Additionally, BN acts as an effective regularizer, often reducing or eliminating the need for Dropout layers [29]. The mathematical formulation of batch normalization can be expressed as follows:

$$\mu\beta = \frac{1}{m}\sum_{i=1}^{m} x^i \quad (10)$$
$$\sigma\frac{2}{\beta} = \frac{1}{m}\sum_{i=1}^{m} (x_1 - \mu\beta)^2 \quad (11)$$
$$x_i = \frac{x_i - \mu\beta}{\sqrt{\sigma\frac{2}{\beta} + \epsilon}} \quad (12)$$
$$y_i = yx_i + \beta = BN_{y,\beta}(x_i) \quad (13)$$

The BNtransform can be added to a network to manipulate any activation. In the notation $yi = BN_{\gamma},\beta(xi)$indicates that the parameters γ and β are to be learned.

3.6. Iris Image Feature Extraction

Following the normalization stage, feature extraction becomes a critical step in iris recognition systems, aiming to capture the unique patterns present in the iris texture. These features are subsequently encoded to form distinctive representations that can be used for matching and identification. The literature highlights a variety of approaches for iris feature extraction, including texture-based, gradient-based, and frequency-based methods[30].

Among these, band-pass decomposition techniques have been widely utilized to generate robust and discriminative biometric templates. Additionally, gradient-based descriptors have been explored for their ability to capture local intensity variations and structural information within the iris region. More recently, deep learning-based approaches, particularly convolutional neural networks, have demonstrated significant potential in automatically learning hierarchical feature representations from normalized iris images. Various architectures have been investigated in prior

 ISSN 2723-6471

studies, each offering different trade-offs between accuracy, computational complexity, and generalization capability. Overall, the choice of feature extraction technique plays a crucial role in determining the effectiveness and reliability of iris recognition systems (see figure 10).

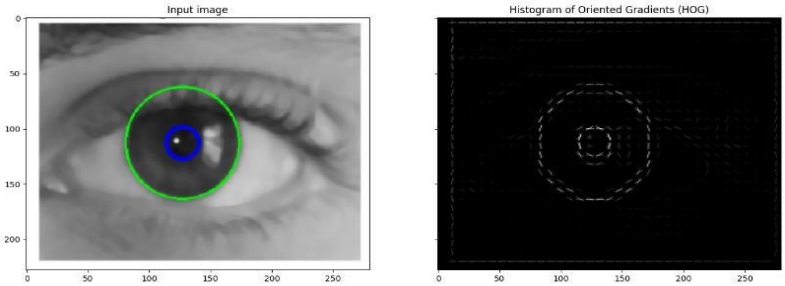

Figure 10. HOG Iris Feature Extraction

Convolutional Neural Networks (CNNs) have been widely adopted in image-based recognition tasks due to their ability to automatically learn hierarchical feature representations from raw data. In the context of iris recognition, prior studies have explored both from-scratch training and transfer learning approaches to improve performance and reduce training complexity. Transfer learning, in particular, has gained significant attention as it enables the reuse of knowledge from large-scale pre-trained models, thereby accelerating convergence and enhancing generalization, especially when limited training data is available. The literature reports the successful application of various well-established CNN architectures, such as VGG-16, ResNet, MobileNet, AlexNet, and InceptionV3, each offering distinct advantages in terms of depth, computational efficiency, and feature extraction capability. These architectures have demonstrated strong performance across various image analysis domains, highlighting the effectiveness of deep learning techniques in extracting discriminative features for biometric recognition tasks [31].

For this study, the modified T-Net architecture serves as our primary feature extraction model. While similar in concept to T-Net incorporates three additional convolutional layers, totalling 19 weight layers (compared to T-Net 16 layers). This deeper architecture with increased parameter capacity processes input images at 224×224 resolution, utilizing a consistent 3×3 convolutional kernel size throughout the network - a design choice that maximizes depth while maintaining minimal receptive fields. Each convolutional operation is followed by ReLU activation, and the network concludes with three fully connected layers. Figure 11 illustrates the analogous T-Net architecture adapted for iris feature extraction [32].

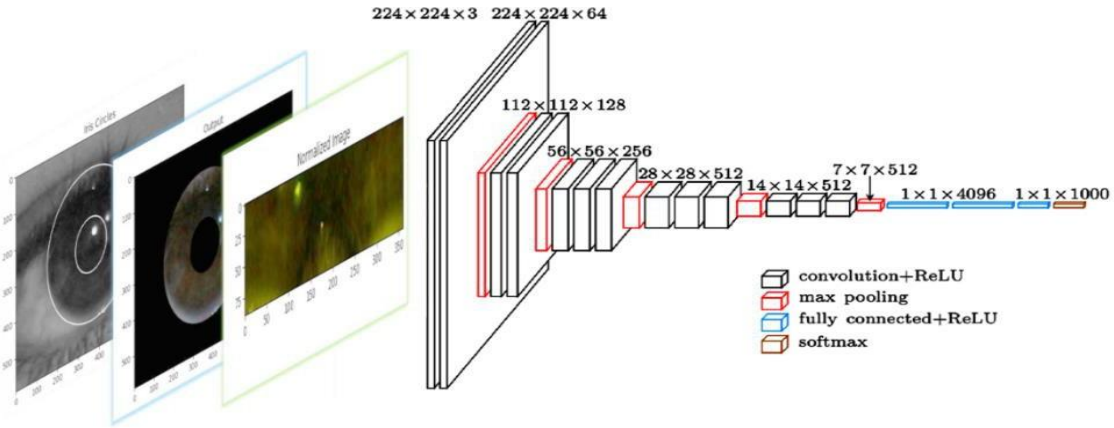

Figure 11. T-Net Iris Feature Extraction Architecture

3.7. Iris Image Pattern Matching

The matching phase in iris recognition systems is a critical step that involves computing similarity scores between input samples and stored templates to support identity verification. This process evaluates the distinctiveness of encoded iris features by comparing representations derived from different images, typically through quantitative similarity or distance measures [33].

The literature highlights a variety of matching strategies, including both binary and feature-based comparison techniques, designed to effectively capture similarities and differences between iris patterns. Feature-based approaches,

in particular, have gained attention for their ability to utilize key point detection and descriptor representation to enhance matching robustness under varying imaging conditions. Additionally, efficient matching algorithms have been explored to ensure scalability and real-time performance in practical biometric systems. Overall, the effectiveness of the matching stage significantly influences the accuracy and reliability of iris recognition, especially when dealing with variations in segmentation quality and image acquisition conditions [34].

3.8. Iris Classification

Current research demonstrates that Deep Convolutional Neural Networks (DCNNs) have emerged as a powerful paradigm across numerous domains. Particularly in computer vision, these architectures have significantly advanced image classification and pattern recognition tasks through their ability to learn hierarchical feature representations [35], [36]. The fundamental strength of CNNs lies in their capacity to automatically extract discriminative spatial features, making them highly suitable for visual analysis application [35] often provide robust foundational frameworks for specialized tasks [36]. The selected architecture for this study follows this proven approach, leveraging:

Input → Conv + ReLU layers (non-linearities) → Pooling layer → Fully connected (dense layer) as Output

The Conv2D layer utilized in this research processes two-dimensional inputs (height and width) with three colour channels. Convolution operations can be applied separately to each channel. The term "filters" refers to the feature detectors that slide across the image, where the quantity of filters determines how many features are extracted. The kernel_size parameter defines the dimensions of these filters for example, a (3, 3) kernel_size means each filter is a 3×3 matrix. The stride specifies how many pixels the filter shifts during each step while scanning the image. Additionally, padding is used to surround the image with zeros, ensuring the output dimensions match the input after convolution.

In the domain of iris recognition, CNN-based approaches have been widely explored to capture distinctive texture patterns that enable reliable differentiation between individuals. The literature indicates that models pre-trained on large-scale datasets, such as ImageNet, often provide strong foundational representations that can be effectively adapted to specialized biometric tasks. This transferability has contributed to improved performance, particularly in scenarios with limited labeled iris data.

Despite these advancements, several challenges remain. Many CNN-based iris recognition systems rely heavily on accurate segmentation, making them sensitive to errors that may propagate and degrade overall performance, especially in unconstrained or non-cooperative environments. Additionally, the dependence on large annotated datasets limits the applicability of such methods in real-world scenarios where data availability is restricted. Furthermore, existing studies often prioritize recognition accuracy while giving less attention to computational efficiency, which is a critical requirement for real-time biometric systems. These limitations highlight the need for more robust, data-efficient, and segmentation-aware approaches in iris recognition research.

4. Results and Discussion

This section presents the findings and evaluation of the proposed iris recognition model, which is based on a Deep Convolutional Neural Network (DCNN). Several experiments were performed to assess the model's accuracy, computational efficiency, and overall performance. The results of these tests are analysed and summarized in detail here.

4.1. Accuracy And Evaluation of The Iris Segmentation Scheme

To evaluate the effectiveness of the proposed iris segmentation method, multiple experiments were conducted using different segmentation techniques on the chosen datasets. The iris images were processed using three approaches: the Hough Transform, T-Net, and Daugman's model. Among these, the T-Net-based segmentation demonstrated superior performance in accurately segmenting iris regions. During training, the U-Net model achieved 94.06% accuracy on the training set and 93.82% on the test set after 150 epochs, which is considered satisfactory given that this was the first implementation of T-Net for iris segmentation in this study. Additionally, four threshold values (0.1, 0.2, 0.3, and 0.4) were applied to enhance foreground extraction based on grayscale intensity, making this method particularly effective for images with high contrast between the iris (foreground) and background. The segmentation accuracy and training loss trends are visually represented in figure 12.

ISSN 2723-6471

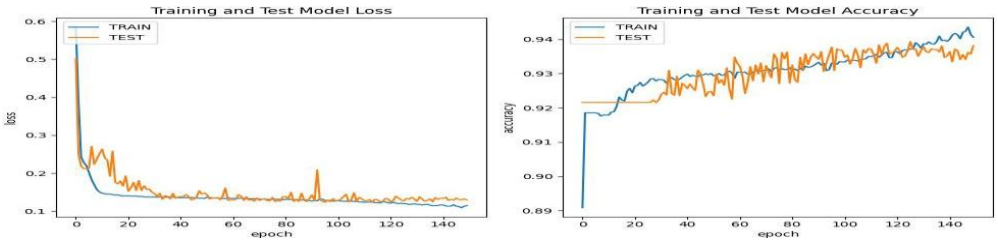

Figure 12. Iris Segmentation accuracy and loss graph

4.2. Evaluation of the Feature Extraction Scheme

To evaluate the feature extraction approach, iris images from the selected datasets were first processed using the proposed segmentation algorithm and then normalized to enhance precision. The study compared multiple feature extraction techniques, including Histogram of Oriented Gradients (HOG), T-Net. An initial experiment was conducted using only 10% of the training images to assess feature extraction performance. The feature extraction layer contained 23,568,898 parameters, representing pre-trained patterns from the ImageNet dataset, indicating that the model had already acquired foundational feature recognition capabilities prior to fine-tuning for iris recognition. This transfer learning approach helped improve efficiency and accuracy in feature extraction [37].

The T-Net model achieved 97.33% training accuracy and 98.23% testing accuracy during the baseline experiment. After hyperparameter refinement and regularization, the optimized T-Net variant achieved improved performance, reaching 97.83% training accuracy and 98.35% testing accuracy, as reported in figure 13.

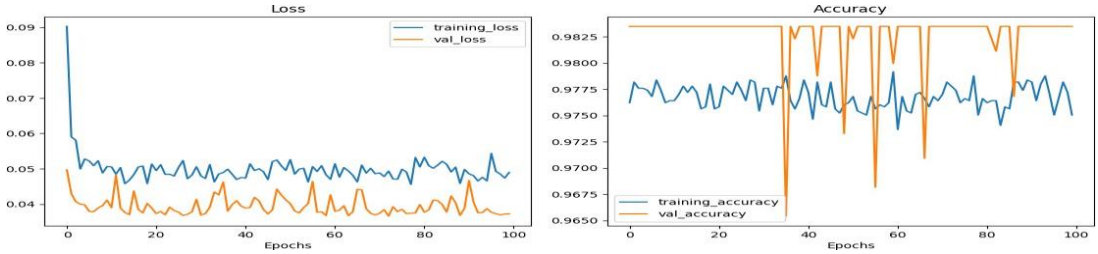

Figure 13. Model training accuracy and loss result on T-Net

4.3. Evaluation of the Iris Classification Scheme

For iris identification, this study employs a Convolutional Neural Network (CNN) architecture. The initial phase involved partitioning the dataset into training and test sets, a crucial step for model development. The data was then converted into batches to optimize processing efficiency. The CNN architecture was initially structured with three consecutive convolution-pooling blocks to enhance feature extraction. Figure 14 displays the model's training progression, showcasing the accuracy and loss curves across epochs, which help evaluate the network's learning dynamics and convergence behaviour.

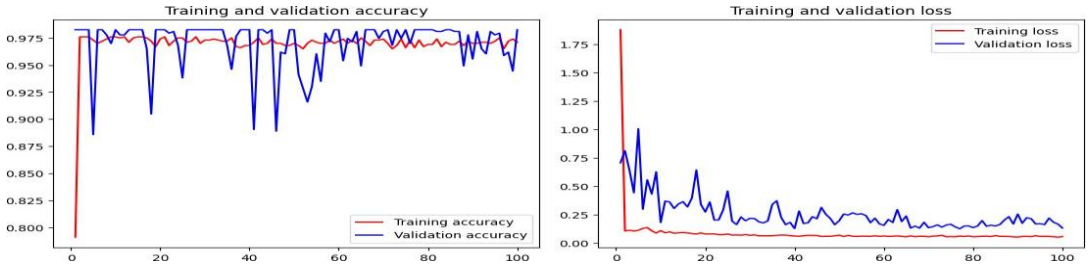

Figure 14. The accuracy and loss curves of model's training performance on CNN

The study leveraged ImageNet [38], [39], [40] for model initialization [41], [42], achieving strong performance with 98.11% training accuracy and 98.35% test accuracy after compilation and training. To further validate the approach, a 3-layer CNN based on T-Net architecture was implemented, yielding comparable results 98.01% training accuracy and 98.35% test accuracy. Figure 15 illustrates the T-Net model's training dynamics, including its accuracy and loss curves, demonstrating stable convergence and effective learning.

ISSN 2723-6471

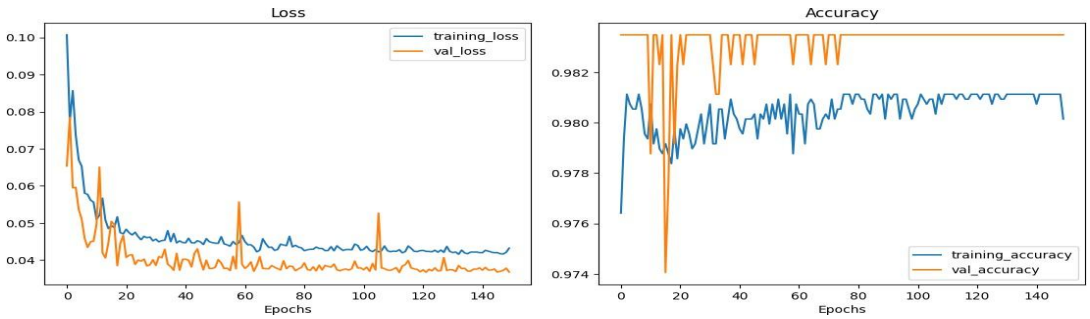

Figure 15. T-Net accuracy and loss performance.

5. Conclusion

This study has presented a robust and segmentation-aware iris recognition framework that tightly integrates a modified T-Net architecture with deep residual feature extraction to enhance both accuracy and computational efficiency. The proposed methodology systematically addresses the critical dependency between segmentation quality and recognition performance, demonstrating that precise iris localization significantly improves feature discriminability and matching reliability. Through comprehensive experiments on multiple public datasets, the framework consistently achieves competitive performance, particularly in scenarios with limited training data, where the combination of segmentation refinement and transfer learning proves highly effective.

Beyond accuracy, this work contributes to the development of a more efficient recognition pipeline by incorporating optimized feature representation and matching strategies, enabling faster processing suitable for real-time biometric applications. The use of enhanced ORB-based matching and hybrid feature extraction further strengthens the system's ability to balance speed and precision, making it practically relevant for deployment in resource-constrained environments.

However, despite these strengths, the system still exhibits limitations when operating under challenging conditions such as extreme occlusion, poor illumination, and severe motion blur, which can negatively impact segmentation quality and, consequently, recognition performance. These limitations highlight the need for further improvements in robustness and generalization.

Future research will therefore focus on enhancing performance under unconstrained acquisition environments by integrating more advanced data augmentation strategies and attention-based deep learning models. Additionally, efforts will be directed toward reducing model complexity to support efficient deployment on embedded and mobile platforms. Finally, the proposed framework can be extended to incorporate multimodal biometric fusion, combining iris recognition with other biometric traits to further improve reliability, security, and scalability in real-world applications.

6. Declarations

6.1. Author Contributions

Conceptualization: H.S., M.S.; Methodology: H.S., T.; Software: M.S., E.T.; Validation: T., H.S.; Formal Analysis: H.S.; Investigation: M.S., E.T.; Resources: T., E.T.; Data Curation: M.S.; Writing – Original Draft Preparation: H.S.; Writing – Review and Editing: T., E.T.; Visualization: E.T.; All authors have read and agreed to the published version of the manuscript.

6.2. Data Availability Statement

The data presented in this study are available on request from the corresponding author.

6.3. Funding

The authors received no financial support for the research, authorship, and/or publication of this article.

6.4. Institutional Review Board Statement

Not applicable.

6.5. Informed Consent Statement

Not applicable.

6.6. Declaration of Competing Interest

The authors declare that they have no known competing financial interests or personal relationships that could have appeared to influence the work reported in this paper.

References

[1] A. Subash, I. Song, I. Lee, and K. Lee, "Integrating user demographic parameters for mouse behavioral biometric based assessment fraud detection in online education platforms," *EURASIP J. Inf. Secur.*, vol. 2025, no. 1, pp. 2–17, 2025, doi: 10.1186/s13635-025-00207-5.

[2] P. M. Than and H. Nguyen, "Efficient multimodal biometric identification via Gabor-enhanced attention networks," *J. Robot. Control*, vol. 6, no. 3, pp. 1175–1186, 2025, doi: 10.18196/jrc.v6i3.26490.

[3] N. Alay and H. H. Al-Baity, "Deep learning approach for multimodal biometric recognition system based on fusion of iris, face, and finger vein traits," *Sensors*, vol. 20, no. 19, pp. 1–17, 2020, doi: 10.3390/s20195523.

[4] Q. Zhang, L. T. Yang, Z. Chen, and P. Li, "A survey on deep learning for big data," *Inf. Fusion*, vol. 20, no. Jan., pp. 146–157, 2018, doi: 10.1016/j.inffus.2017.10.006.

[5] R. A. Asmara, M. Ridwan, and G. Budiprasetyo, "Haar cascade and convolutional neural network face detection in client-side for cloud computing face recognition," *IEEE Access*, vol. 2021, no. Oct., pp. 1–10, 2021, doi: 10.1109/IEIT53149.2021.9587388.

[6] S. Umer, B. C. Dhara, and B. Chanda, "Iris recognition using multiscale morphologic features," *Pattern Recognit. Lett.*, vol. 65, no. Jan., pp. 67–74, 2021, doi: 10.1016/j.patrec.2015.07.008.

[7] Y. Zhu, P. Wu, H. Fang, Y. Zhang, and F. Xie, "Key technologies and applications of cloud energy storage," *IOP Conf. Ser. Mater. Sci. Eng.*, vol. 2022, no. Jun., pp. 1–10, 2022, doi: 10.1088/1757-899X/768/6/06201.

[8] O. N. Kadhim and M. H. Abdulameer, "A multimodal biometric database and case study for face," *Bull. Electr. Eng. Inform.*, vol. 13, no. 1, pp. 677–685, 2024, doi: 10.11591/eei.v13i1.6605.

[9] A. Negoitescu, "Intelligent human iris recognition system based on deep learning," *IEEE Access*, vol. 2025, no. Jan., pp. 15–23, 2025, doi: 10.5220/0013037000003890.

[10] R. Smit, A. Ayala, G. Kadijk, and P. Buekenhoudt, "Excess pollution from vehicles—A review and outlook on emission controls, testing, malfunctions, tampering, and cheating," *Sustainability*, vol. 17, no. 12, pp. 1–58, 2025, doi: 10.3390/su17125362.

[11] S. Gang, N. Fabrice, D. Chung, and J. Lee, "Character recognition of components mounted on printed circuit board using deep learning," *Sensors*, vol. 21, no. 9, pp. 1–21, 2021, doi: 10.3390/s21092921.

[12] R. Parashar and S. Joshi, "Comparative study of iris databases and UBIRIS database for iris recognition methods for non-cooperative environment," *Int. J. Eng. Res. Technol.*, vol. 1, no. 5, pp. 2–7, 2022.

[13] D.-L. Nguyen, M. D. Putro, and K.-H. Jo, "Human eye detector with light-weight and efficient convolutional neural network," *Adv. Comput. Collect. Intell.*, vol. 1287, no. Jan., pp. 1–11, 2020, doi: 10.1007/978-3-030-63119-2_16.

[14] Y. Wang, D. Shi, and W. Zhou, "Convolutional neural network approach based on multimodal biometric system with fusion of face and finger vein feature," *Sensors*, vol. 22, no. 16, pp. 2–15, 2022, doi: 10.3390/s22166039.

[15] Y. Sun and Y. Hua, "Image preprocessing of iris recognition," *IEEE Access*, vol. 2018, no. Oct., pp. 1–10, 2018, doi: 10.1109/ICAM.2018.8596533.

[16] R. T. Mohammed, H. Kaur, B. Alankar, and R. Chauhan, "Recognition of human iris for biometric identification using Daugman's method," *IET Biometrics*, vol. 11, no. 4, pp. 304–313, 2021, doi: 10.1049/bme2.12074.

[17] J. Liu, S. Liu, Z. He, Y. Xiao, G. Cui, and PengPeng, "A shield segment bolt detection and localization method based on ellipse detection," *IEEE Access*, vol. 13, pp. 89208–89221, 2025, doi: 10.1109/ACCESS.2025.3566675.

[18] A. Kumar, "Insights on 'complex-valued iris recognition network'," *IEEE Trans. Pattern Anal. Mach. Intell.*, vol. 47, no. 3, pp. 2232–2236, 2024, doi: 10.1109/TPAMI.2024.3489775.

[19] A. S. Hassanein, S. Mohammad, M. Sameer, and M. E. Ragab, "A survey on Hough transform, theory, techniques and applications," *arXiv*, vol. 2021, no. Feb., pp. 1–18, 2021, doi: 10.48550/arXiv.1502.02160.

[20] T. Mansfield, G. Kelly, D. Chandler, and J. Kane, "Biometric product testing final report," *IEEE Access*, vol. 2021, no. Jan., pp. 1–20, 2021, doi: 10.24406/publica-45.

[21] J. Daugman, "How iris recognition works," *IEEE Trans. Circuits Syst. Video Technol.*, vol. 14, no. 1, pp. 21–30, 2021, doi: 10.1016/B978-0-12-374457-9.00025-1.

[22] Norhikmah, A. Lutfhi, and Rumini, "The effect of layer batch normalization and dropout of CNN model performance on facial expression classification," *Int. J. Informatics Vis.*, vol. 6, no. 2-2, pp. 481–488, 2021, doi: 10.30630/joiv.6.2-2.921.

[23] H. Tabrizchi, A. Mosavi, Z. Vamossy, and A. R. Varkonyi-Koczy, "Densely connected convolutional networks (DenseNet) for diagnosing coronavirus disease (COVID-19) from chest X-ray imaging," *IEEE Access*, vol. 2021, no. Jun., pp. 1–10, 2021, doi: 10.1109/MeMeA52024.2021.

[24] P. N. Pateriya, P. P. Jain, P. K. P. Niveditha, V. Tiwari, and S. Vishwakarma, "Deep residual networks for image recognition," *IEEE Access*, vol. 2023, no. Sep., pp. 10742–10747, 2023, doi: 10.15680/IJIRCCE.2023.1109026.

[25] Herman, Y. J. Kumar, S. Y. Wee, and V. K. Perhakaran, "Lightweight deep learning model with ResNet14 and spatial attention for anterior cruciate ligament diagnosis," *Int. J. Adv. Intell. Inform.*, vol. 11, no. 3, pp. 367–378, 2025, doi: 10.26555/ijain.v11i3.2055.

[26] S. Santurkar, D. Tsipras, A. Ilyas, and A. Madry, "How does batch normalization help optimization?" *arXiv*, vol. 2018, no. May, pp. 1–11, 2018, doi: 10.48550/arXiv.1805.1160.

[27] M. Omran and E. N. AlShemmary, "An iris recognition system using deep convolutional neural," *J. Phys. Conf. Ser.*, vol. 1530, no. Jan., pp. 1–11, 2020, doi: 10.1088/1742-6596/1530/1/012159.

[28] T. Surasak, I. Takahiro, C.-H. Cheng, C.-E. Wang, and P.-Y. Shen, "Histogram of oriented gradients for human detection in video," *IEEE Access*, vol. 2018, no. May, pp. 1–10, 2018, doi: 10.1109/ICBIR.2018.8391187.

[29] W. Zhou, S. Gao, L. Zhang, and X. Lou, "Histogram of oriented gradients feature extraction from raw Bayer pattern images," *IEEE Trans. Circuits Syst. II*, vol. 67, no. 5, pp. 946–950, 2020, doi: 10.1109/TCSII.2020.2980557.

[30] R. Gonzalez, R. Woods, and S. Eddins, "Digital image processing using MATLAB," *Gatesmark Publ.*, vol. 2020, no. Jan., pp. 17–46, 2020.

[31] M. S. M. Khan, M. Ahmed, R. Z. Rasel, and M. M. Khan, "Cataract detection using convolutional neural network with VGG-19 model," in *IEEE World AI IoT Congress*, Seattle, WA, USA, 2021, doi: 10.1109/AIIoT52608.2021.

[32] G. Zhao, Y. Shen, C. Zhang, Z. Shen, Y. Zhou, and H. Wen, "RGBE-gaze: A large-scale event-based multimodal dataset for high frequency remote gaze tracking," *IEEE Trans. Pattern Anal. Mach. Intell.*, vol. 47, no. 1, pp. 601–615, 2025, doi: 10.1109/TPAMI.2024.3474858.

[33] X. Zhang, Y. Sugano, M. Fritz, and A. Bulling, "Appearance-based gaze estimation in the wild," in *IEEE Conf. Comput. Vis. Pattern Recognit.*, Boston, MA, USA, 2019, doi: 10.1109/CVPR.2015.7299081.

[34] Z. Haliche, K. Hammouche, O. Losson, and L. Macaire, "Fuzzy color aura matrices for texture image segmentation," *J. Imaging*, vol. 8, no. 9, pp. 1–20, 2022, doi: 10.3390/jimaging8090244.

[35] D. J. Mandal, H. Deborah, T. L. Tobing, M. Janiszewski, J. W. Tanaka, and A. Lawrance, "Comprehensive evaluation of ImageNet-trained CNNs for texture-based rock classification," *IEEE Access*, vol. 12, pp. 94765–94783, 2024, doi: 10.1109/ACCESS.2017.DOI.

[36] F. Becker, A. Drichel, C. Muller, and T. Ertl, "Interpretable visualizations of deep neural networks for domain generation algorithm detection," in *IEEE Symp. Visualization for Cyber Security*, Salt Lake City, UT, USA, 2020, doi: 10.1109/VizSec51108.2020.00007.

[37] M. A. Rahman, L. E. Ali, S. Kumar, Mistry, A. Mukherjee, and M. Z. Islam, "Distant iris recognition through machine learning models with deep feature transfer for human identification," *J. Innov. Image Process.*, vol. 7, no. 3, pp. 840–860, 2025, doi: 10.36548/jiip.2025.3.014.

ISSN 2723-6471

[38] N. Ying, Y. Lei, T. Zhang, S. Lyu, S. Chen, Z. Liu, Y. Feng, Y. Zhao, and G. Zhang, "CPIA dataset: A large-scale comprehensive pathological image analysis dataset for self-supervised learning pre-training," *Biomed. Signal Process. Control*, vol. 110, pp. 1–11, 2025, doi: 10.1016/j.bspc.2025.108148.

[39] P. Patil and K. Vasanth, "Iris recognition using local and global iris image moment features," in *IEEE*, vol. 1, pp. 1–5, 2019, doi: 10.1109/i-PACT44901.2019.8960219.

[40] E. Jalilian, G. Wimmer, A. Uhl, and M. Karakaya, "Deep learning based off-angle iris recognition," in *IEEE Int. Conf. Acoustics, Speech Signal Process.*, Singapore, 2022, doi: 10.1109/ICASSP43922.2022.9746090.

[41] Suwarno, Y. Christian, K. Yoputra, and Y. Estrada, "Exploring machine learning to support software managers' insights on software developer productivity," *J. Appl. Data Sci.*, vol. 6, no. 3, pp. 1504–1524, 2025, doi: 10.47738/jads.v6i3.661.

[42] C. Wang, W. He, X. Yan, P. Chen, and J. Wang, "L-YOLO-HR: Implementing lightweight and efficient pavement distress detection by enhancement of the spatial information extractions of high-resolution features," *Eng. Res. Express*, vol. 7, pp. 1–19, 2025, doi: 10.1088/2631-8695/ae0f01.